

AD-A227 407

Environmental Conditions Associated with the Dallas Microburst Storm Determined from Satellite Soundings

GARY ELLROD

Satellite Applications Laboratory (NOAA/NESDIS) Washington, D.C.

(Manuscript received 13 July 1988, in final form 15 May 1989)

DTIC
ELECTE
OCT 05 1990

D

ABSTRACT

The thermodynamic structure of the troposphere in the vicinity of the microburst storm at Dallas-Ft. Worth Airport (DFW), Texas on 2 August 1985 is described. The analysis was based principally on a set of vertical soundings from the Visible and Infrared Spin Scan Radiometer (VISSR) Atmospheric Sounder (VAS) onboard the *Geostationary Operational Environmental Satellite* (GOES), valid about 1 h before the occurrence of peak surface winds. Convection in the DFW area developed in a gradient of stability on the west side of a tongue of low lifted index and high precipitable water. The lapse rates in the 850 mb–700 mb layer were large (8° – $9^{\circ}\text{C km}^{-1}$). Vertical profiles of VAS data showed that DFW was in a transition zone in which conditions became drier at all levels and slightly warmer near 500 mb to the south and southwest. The midlevel warming reduced the buoyant energy available above cloud base, thus acting as a capping mechanism for the unstable, northward-moving low-level air. The potential instability was released in the vicinity of DFW by low-level convergence, caused in part by an outflow boundary from earlier convection. The storm had characteristics of both the wet and dry types of microbursts based on current models. There was a large decrease with height in total static energy (inferred from equivalent potential temperatures) from the surface to 700 mb, resulting in a source of potentially cool air fairly close to the surface.

1. Introduction

On 2 August 1985, a commercial airliner crashed while attempting to land in a thunderstorm at Dallas-Ft. Worth Airport (DFW), resulting in the loss of 133 lives. The prime factor in the accident was severe microburst wind shear on the final approach path, a situation aggravated by poor visibility due to heavy rains. Surface winds gusted to 23 m s^{-1} (45 kt) shortly after the time of the accident (about 2306 UTC) and 36 m s^{-1} (70 kt) 12 minutes later. Many aspects of this storm, based on flight recorder data, surface reports, radar and satellite imagery, have been previously described (Fujita 1986; Caracena et al. 1986; Proctor 1988).

The storm was small but intense. Radar showed a cell less than 10 km in diameter near the north end of the runway which intensified to more than 40 dbz about 10 min after it developed (Caracena et al. 1986). Small, severe convective storms similar to the one that occurred at DFW have been implicated in other aircraft accidents (e.g., Fujita 1983; Fujita and Caracena 1977). They present a formidable challenge to aviation meteorologists because they are difficult to forecast at a specific location and have a relatively short life cycle.

Their radar and satellite signatures are often subtle or nonexistent.

A type of remotely sensed data which may be helpful in the analysis and short range forecasting of such convective storms are vertical soundings (also known as retrievals) derived from radiance measurements from the *Geostationary Operational Environmental Satellite* (GOES) Visible and Infrared Spin Scan Radiometer (VISSR) Atmospheric Sounder (VAS). On 2 August 1985, soundings were produced at 1418, 1648, and 2218 UTC from the GOES-6, the only operational geostationary satellite at the time. The 2218 UTC set of retrievals observed the north-central Texas region about one h prior to the accident, and will be the data period stressed in this analysis. The normal time interval between VAS soundings is about 90 min. The long periods of elapsed time between VAS datasets on this data ($5\frac{1}{2}$ h for the latter two) was unfortunate, and did not allow a determination of either the rapidity of changes which occurred or how far in advance of the microburst event those changes took place. Despite this shortcoming, some important features and trends were evident in these data. This paper will discuss many aspects of the DFW storm's environmental conditions deduced from the sounding data, such as atmospheric stability, moisture, and buoyant energy. Important surface-forcing mechanisms were analyzed from available surface and satellite data. The conditions relating

Corresponding author address: Gary Ellrod, Satellite Application Laboratory, NOAA/NESDIS, Washington, DC, 20233.

to the DFW storm will be compared to existing conceptual models of microburst environments.

2. VAS data analysis

The VAS instrument on GOES obtains radiance measurements in 12 spectral bands, three of which are water vapor absorption channels. A summary of the characteristics of each channel is shown in Table 1. The GOES has three basic operating modes: 1) the VISSR mode in which visible and infrared (IR) images are produced, 2) Multispectral Image (MSI) mode in which data are obtained from two additional channels besides VISSR, and 3) the VAS Dwell Sounding (DS) mode in which all 12 channels are sampled.

VAS retrievals are derived using the following procedure: An initial profile of temperature and moisture is obtained from a 12-h forecast numerical model (for this case the limited area fine mesh or LFM). These profiles are modified by use of the satellite radiance measurements in the matrix inversion of a perturbation form of the radiative transfer equations. The equations yield a simultaneous solution of temperature and moisture. Detailed explanations of the processing techniques are available in the literature (Smith 1983; Menzel et al. 1983; Smith and Woolf 1984; Menzel and Hayden 1986).

The VAS infrared sensors have a maximum horizontal resolution of 7 km in seven of the channels and 14 km in the remaining five channels (Table 1). The radiances are spatially averaged for an 11×11 array, resulting in a rectangular-shaped sample with sides of about 80 km in a east-west direction and 100 km in north-south direction at the latitude of central Texas. Additionally, the radiances are temporally averaged by multiple sampling along each scan line (referred to as spin budgets). The effect of this process is to reduce instrument noise, which varies from channel to channel.

Sounding retrievals are processed only for clear or partly cloudy fields of view (FOV). The determination of cloudy pixels is accomplished by comparisons of the

11- μ channel temperatures with an objective analysis of the surface skin temperatures, obtained from surface observations (Hayden et al. 1984). If the warmest 11- μ value in a sample is more than 10°C colder than the surface temperature at that location, the sample is assumed to be cloudy and is rejected. For partly cloudy samples, pixel-to-pixel slope tests are used to identify clear pixels. The latter procedure results in an increase of about 10% in the number of usable retrievals. Despite these tests, however, some cloud-contaminated samples undoubtedly slip through, due to cloud elements which are smaller than the FOV.

While the spatial resolution provided by VAS is much better than conventional radiosonde coverage, the vertical resolution is not as good, due to the broad response functions for most of the channels. For this reason, VAS soundings cannot resolve shallow inversions or moist layers, especially at low levels (<700 mb). The retrieved soundings tend to smooth these features out. The main contributions to low-level parameters such as surface temperatures and moisture are provided by the extrapolation of hourly surface observations or numerical model output.

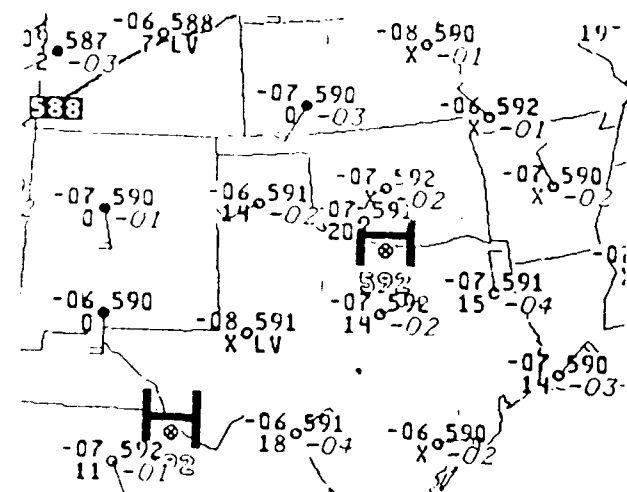
Derived sounding products include temperature (T), dew point temperature (T_d) and geopotential height (Z) at most standard pressure levels, and layer mean products such as lifted index (LI) and total precipitable water (PW). The accuracy of these parameters has been documented (Wade et al. 1985; Montgomery and Uccellini 1985). Root mean square (RMS) errors are typically 1°–3°C for T , but can be as much as 8°C for T_d . Horizontal variations of the derived products (gradients) and vertically integrated quantities (such as lifted index) are considered more useful operationally (Montgomery and Uccellini 1985; Wade et al. 1985; Mills and Hayden 1983; Smith et al. 1982). Nevertheless, significant vertical variations in temperature and moisture should be detectable in many situations.

The VAS data were displayed and analyzed on the Man Computer Interactive Data Access Systems

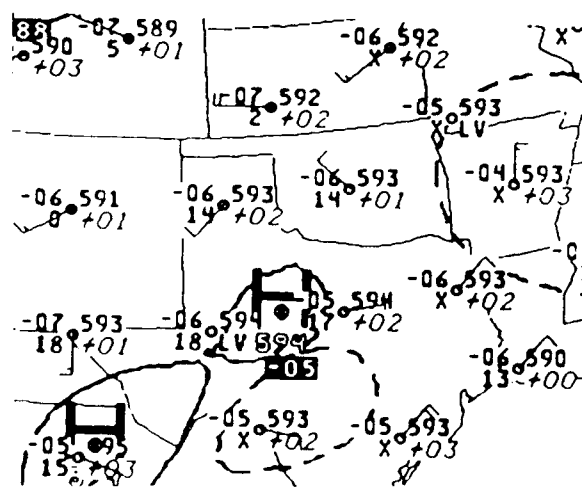
TABLE 1. Characteristics of VAS channels.

| Channel number | Wavelength (μ) | Peak response (μ) | 10%–90% Radiance layer (mb) | Purpose for sounding | Main absorbing gas | Maximum resolution (km) |
|----------------|----------------------|-------------------------|-----------------------------|----------------------|-----------------------------------|-------------------------|
| 1 | 14.7 | 70 | 4–120 | temp | CO ₂ | 14 |
| 2 | 14.5 | 125 | 4–225 | temp | CO ₂ | 14 |
| 3 | 14.3 | 200 | 15–475 | temp | CO ₂ | 7 |
| 4 | 14.0 | 500 | 40–900 | temp | CO ₂ | 7 |
| 5 | 13.3 | 920 | 420–sfc | temp | CO ₂ | 7 |
| 6 | 4.5 | 850 | 520–sfc | temp + cloud | N ₂ O | 14 |
| 7 | 12.6 | 1000 | 720–sfc | moisture | H ₂ O | 7 |
| 8 | 11.2 | sfc | 920–sfc | surface | H ₂ O | 7 |
| 9 | 7.2 | 600 | 110–820 | moisture | H ₂ O | 7 |
| 10 | 6.7 | 400 | 240–620 | moisture | H ₂ O | 7 |
| 11 | 4.4 | 300 | 7–1000 | temp + cloud | N ₂ O, CO ₂ | 14 |
| 12 | 3.9 | sfc | sfc–sfc | surface | H ₂ O | 14 |

(McIDAS) (Suomi et al. 1983) at both the University of Wisconsin-Madison, and the World Weather Building in Camp Springs, Maryland. In addition to the normally derived sounding products, equivalent potential temperature (θ_e) was derived and analyzed for each pressure level. Lapse rates were determined for the 850–700 mb and 850–500 mb layers. Vertically integrated buoyant energy calculations were also produced for each retrieval. For analyses involving parameter changes between pressure levels or time periods, the data were interpolated from the sounding locations to grid points spaced at about 1-deg intervals, using a Barnes objective analysis routine. The contouring routine interpolates across regions devoid of data, such as the absence of VAS retrievals in cloudy areas. In some cases, contours were manually drawn



a. 1200 UTC 2 AUG 85



b.0000 UTC 3 AUG 85

FIG. 1. 500 mb analyses at (a) 1200 UTC 2 August 1985 and (b) 0000 UTC 3 August 1985.

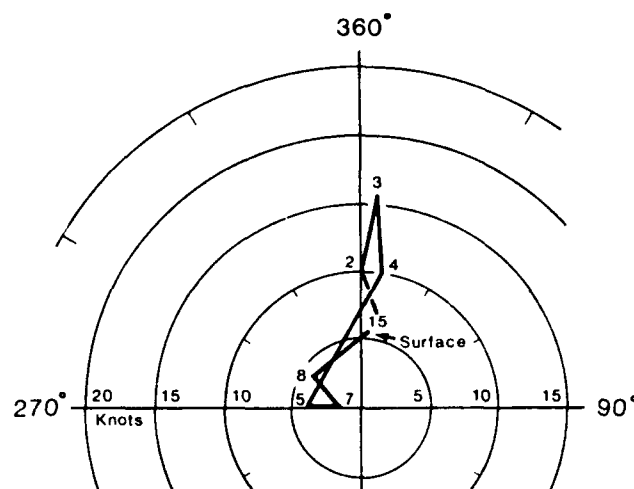


FIG. 2. Hodograph showing vertical wind profile at Stephenville, Texas valid 0000 UTC 3 August 1985. Numbers refer to standard pressure levels (i.e., 8 = 850 mb).

to highlight features smoothed out by the objective analyses.

3. Synoptic setting

On 2 August 1985, the 500 mb analyses (Fig. 1) showed a large, weak anticyclone covering the Southern Plains of the United States. Light easterly flow persisted over north-central Texas through the day, as the upper-level high remained quasistationary. A hodograph for Stephenville, Texas (SEP, located about 150 km southwest of DFW) valid at 0000 UTC 3 August 1985 (Fig. 2), showed light southerly flow at the surface, east to southeast flow at midlevels, becoming southerly above 500 mb. Wind speeds were $\leq 8 \text{ m s}^{-1}$ ($\leq 16 \text{ kt}$) at all levels. For this reason, the downward transport of horizontal momentum did not contribute significantly to the observed surface wind gusts. Also, the weak shear environment precluded the development of long-lived convection on this day.

At the surface, a weak, shallow quasi-stationary front was analyzed from south-central Oklahoma to north-central Louisiana (Fig. 3). This boundary separated very hot, moist southerly flow originating from the Gulf of Mexico with slightly cooler but very humid easterly flow to the north of the front. The frontal analysis throughout this day was complicated by prefrontal troughs and outflow boundaries resulting from convective downdrafts. Mesoscale effects were thus dominant over the synoptic scale. Surface dew point temperatures decreased slowly westward from 18°–21°C (65°–70°F) in central Texas to minima of 13°–16°C (55°–60°F) in the High Plains.

4. VAS imagery

GOES visible imagery at 2301 UTC (Fig. 4) shows an organized line of convection developing over north-

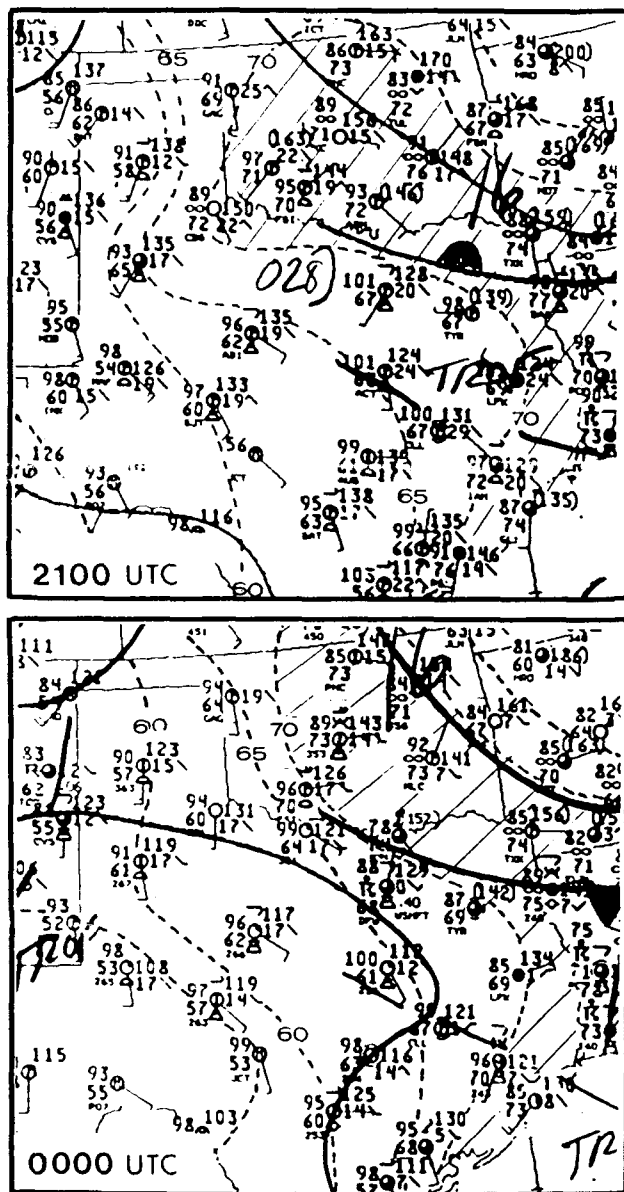


FIG. 3. NMC surface analysis at 2100 UTC 2 August 1985 (top) and 0000 UTC, 3 August 1985 (bottom). Dashed lines are isodrosotherms at intervals of 5°F. The cross-hatched area shows where $T_d > 70^\circ\text{F}$.

central Texas. Evidence of this activity was first observed at 2231 UTC. The linear organization suggests the presence of an outflow boundary or other mesoscale convergence line which often initiates convection (Purdum 1971). Inspection of earlier visible imagery showed the presence of one or two cumulonimbus clouds east of DAL which had dissipated by 2131 UTC. The dissipation of convection usually results in some evaporational cooling at low levels and differential heating around the edge of persistent anvil cirrus debris. The wind shift to an easterly direction at DFW around 2300 UTC and the nearly circular clear zone east of DAL (Fig. 4) are further evidence that an outflow

boundary was present, surrounding a weak mesohigh. Another mesohigh is also shown by the clear zone northwest of FTW. Farther to the north and east, much larger storms lurked along the Oklahoma border, extending southeastward into east Texas.

The convective cells grew rapidly from 2230–2300 UTC, as shown by rather lengthy shadows to the east in Fig. 4. The rapid rate of development, plus the normal processing time necessary to receive satellite imagery via telephone line transmission, resulted in little or no advance warning from the 30-min interval visible imagery. The availability of rapid scan (5 min) imagery would have been of great benefit in providing frequent, qualitative measures of the growth of these cells, such as changes in cloud brightness, shadow length and IR temperatures. Unfortunately, simultaneous rapid scan imagery and sounding retrievals are not possible with the current GOES. The GOES I-M series, to become operational in the 1990s, will have this capability, since the sounder and imager will be independent (Komajda and McKenzie 1987).

The smoothed, enhanced infrared (IR) image in Fig. 4 dramatizes the insignificant appearance of the DFW storm compared to its menacing neighbors to the north and east. Analysis of the IR data showed minimum cloud top temperatures (CTT) of about -14°C as opposed to a range of -65° to -70°C near the Red River along the Oklahoma border. A portion of this difference can be accounted for by the inability of the GOES to obtain accurate IR temperatures for small convective clouds. This is due to the cloud top not completely filling the FOV, and a lag in the response of the VISSR instrument. IR images an hour later (when anvil cloud debris from these storms had expanded) showed CTTs near -50°C , which is possibly more representative of the 2301 UTC conditions. The colder CTT would have resulted in a cloud top height of about 12.2 km (40 000 ft). The improved resolution of IR imagery (4 vs 8 km currently) planned for the GOES I-M series (Komajda and McKenzie 1987) should greatly enhance our ability to monitor small convective storms.

Another capability which could have been useful in this case (although only one GOES was operational at the time) is stereoscopic imagery (Hasler et al. 1982), obtained from simultaneous imaging by two satellites at different viewing angles, such as GOES-East and GOES-West. It is believed that accurate growth rates of convective clouds can be obtained from stereo imagery (Mack et al. 1982), since the cloud top heights are determined from geometry and not radiometry. This capability is not expected to be operationally available in the near future, though.

Imagery from the VAS water vapor channels is often useful in qualitative assessment of mid- or upper-level moisture conditions in the preconvective environment (Petersen et al. 1984). The enhanced $6.7\text{-}\mu$ water vapor image at 2218 UTC is shown in Fig. 5. Darker regions in the image represent areas where there is minimal

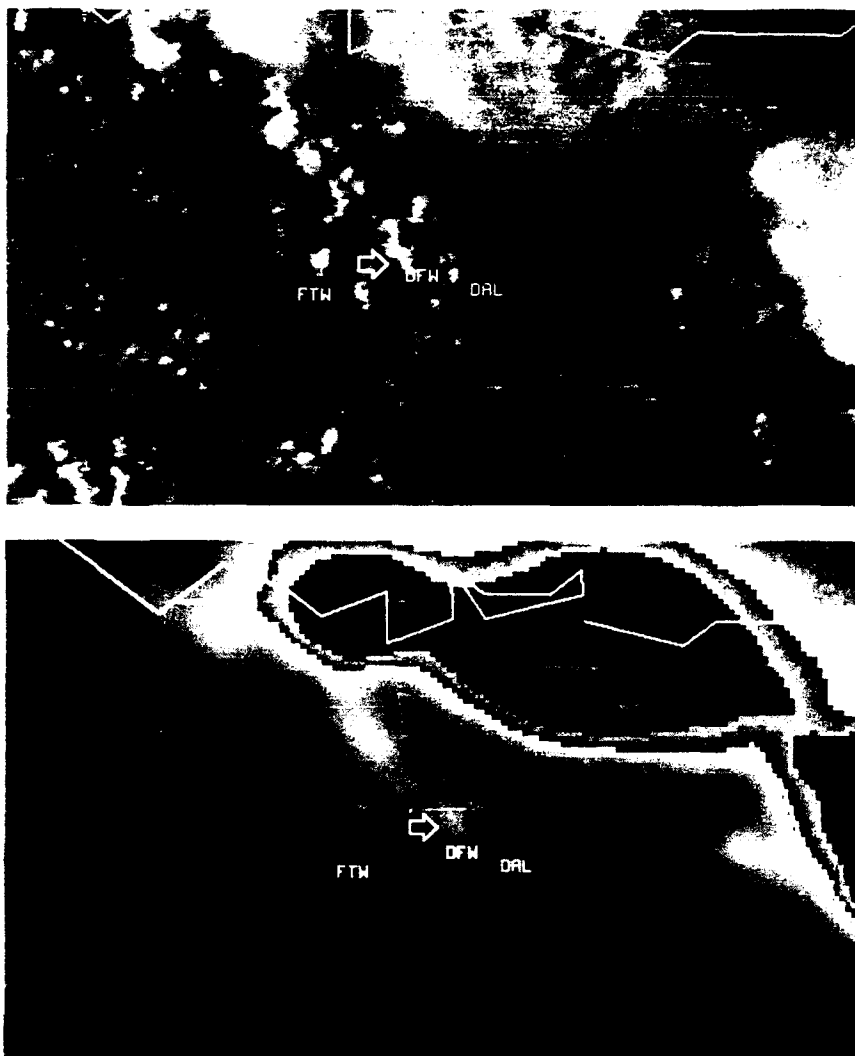


FIG. 4. GOES visible image (top) and smoothed infrared image (bottom) at 2301 UTC, 2 August 1985. Storms which affected DFW are shown by arrow. Infrared image is enhanced with operational "MB curve." Outer gray step contour shows temperature of -33°C , and black is -60°C .

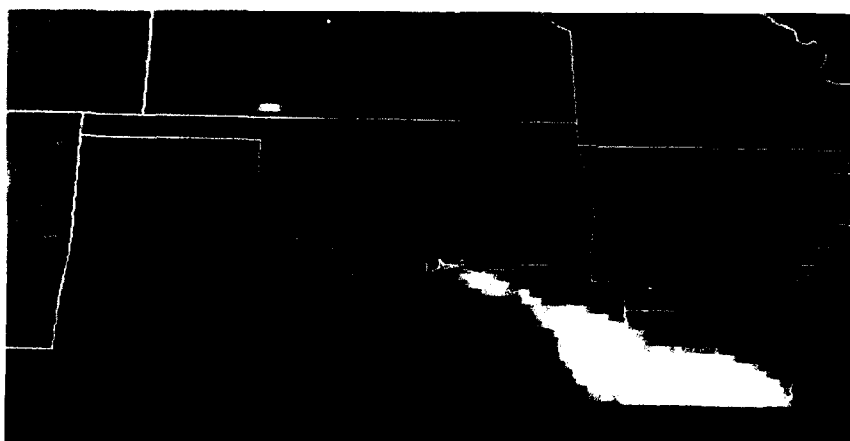


FIG. 5. Enhanced image from VAS 6.7μ moisture channel at 2218 UTC 2 August 1985. Arrow shows dry zone just to the south of DFW.

| | |
|-----------------|-------------------------------------|
| For | |
| GRA&I | <input checked="" type="checkbox"/> |
| MB | <input checked="" type="checkbox"/> |
| anced | <input type="checkbox"/> |
| ication | <input type="checkbox"/> |
| Distribution/ | |
| liability Codes | |
| Avail and/or | |
| Special | |
| A-1 20 | |

moisture through a deep layer in the middle and high troposphere, which allows radiance from warmer low levels to reach the satellite sensor. A broad band of relatively dry air extended from the Texas panhandle eastward to southern Arkansas and northern Louisiana. DFW was situated approximately in the middle of this dry band. The $7.2\ \mu$ channel image (not shown), which is sensitive to moisture in the 500–700 mb layer, had a similar appearance. This subtle dark zone, which was also evident in earlier water vapor images, had apparently developed in situ as a result of sinking related to the mid and upper level anticyclone.

5. Quantitative VAS analyses

a. Lifted index

Analyses of LIs derived from VAS at 1648 and 2218 UTC are shown in Fig. 6. The DFW storm developed on the western fringe of a tongue of instability which

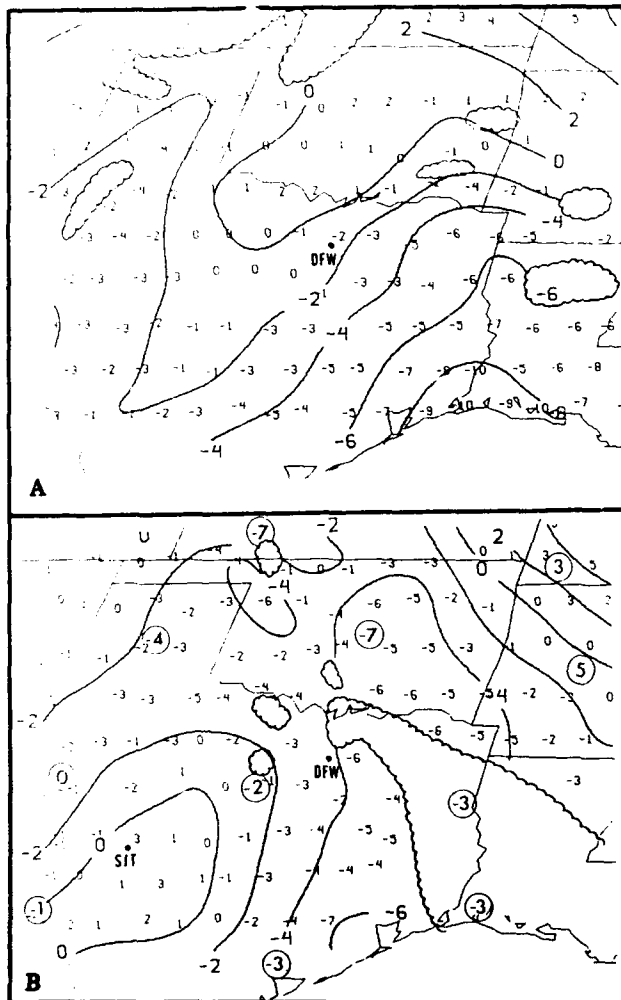


FIG. 6. VAS-derived lifted index ($^{\circ}\text{C}$) at (a) 1648 UTC and (b) 2218 UTC. Radiosonde lifted index values for 0000 UTC 3 August 1985 are shown by circled numbers. Scalloped areas show approximate location of deep convection or middle and high cloudiness.

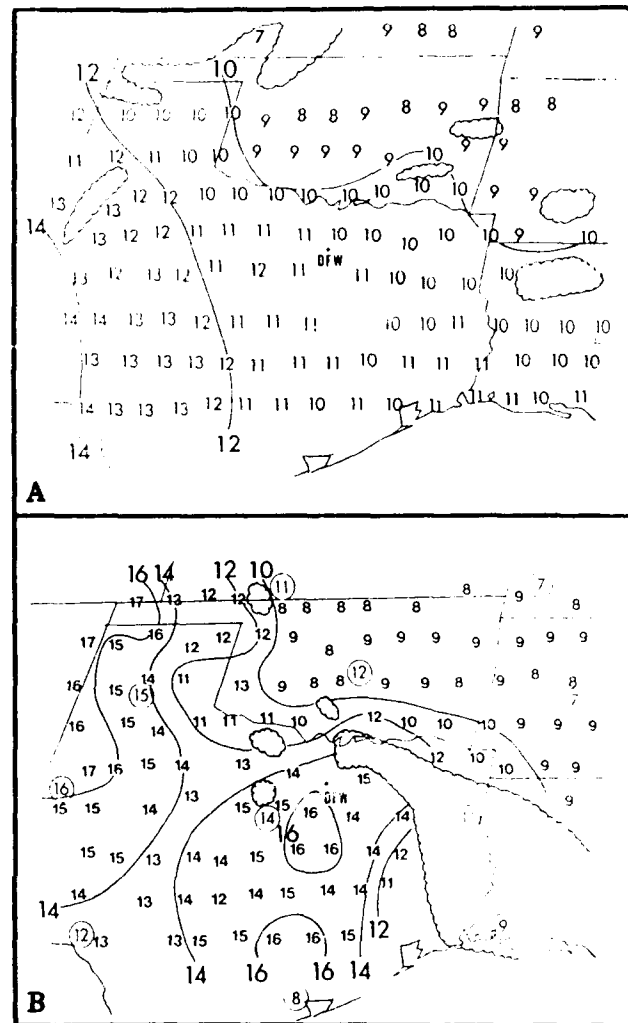


FIG. 7. As in Fig. 6 except for lapse rates ($^{\circ}\text{C}$) for the 850–700 mb layer.

spread northwestward during the afternoon from the Louisiana and southeast Texas coasts. Deep convection developed within the unstable region along the stationary front where VAS-derived LIs were a minimum of -6°C . A strong gradient of LI over central Texas at 1648 UTC had moved over the DFW area by 2218 UTC, and had become reoriented along a north-south line, nearly parallel to the low-level flow. The gradient became a little more pronounced as a result of stabilization to the southwest of DFW [LI increased to about $+3^{\circ}\text{C}$ near San Angelo (SJT)] and destabilization to the east and southeast. The LI values determined from radiosonde data at 0000 UTC 3 August (the circled numbers in Fig. 6) showed generally good agreement with the VAS data.

b. Lapse rates

An analysis of the 850–700 mb lapse rates ($^{\circ}\text{C}$) at 1648 and 2218 UTC is shown in Fig. 7. High lapse

rates in the subcloud layer are believed to be an important factor in the generation of strong convective downdrafts (Srivastava 1987). An extensive study of numerous VAS-derived convective indices (Kitzmler and McGovern 1988) has shown that lapse rates contained the most predictive information for determining severe storm potential using VAS data. The lapse rate analysis at 1648 UTC was featureless, with values increasing steadily westward to a maximum of $13^{\circ}\text{--}14^{\circ}\text{C}$ in the drier high elevations of west Texas and New Mexico. By 2218 UTC, lapse rates of $13^{\circ}\text{--}16^{\circ}\text{C}$ ($8^{\circ}\text{--}9^{\circ}\text{C km}^{-1}$) were widespread from east central Texas westward, but with a well-defined maximum of 16°C just to the south of DFW. The values at 2218 UTC are similar to those obtained from radiosondes. Results from the Joint Airport Weather Studies (JAWS) at Denver indicated that 700–500 mb lapse rates $> 8^{\circ}\text{C km}^{-1}$ related to a high probability of microbursts (Carcena and Flueck 1987). The 850 mb–700 mb layer in north Texas is analogous, considering the differences in terrain height and cloud bases. While microbursts are possible with lapse rates from $6^{\circ}\text{--}8^{\circ}\text{C km}^{-1}$, very heavy rainfall or the presence of ice are required (Srivastava 1987). The 700–500 mb lapse rates (not

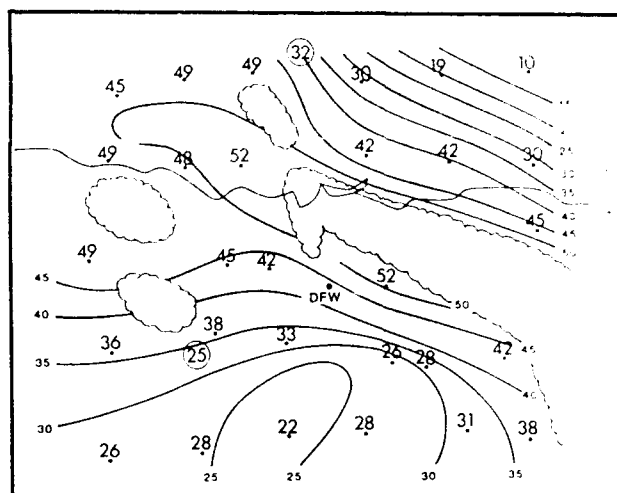


FIG. 9. Relative humidity (%) for a layer centered at 500 mb derived from VAS temperatures and dew points at 2218 UTC. Radiosonde values are circled.

shown) were slightly weaker ($6^{\circ}\text{--}7^{\circ}\text{C km}^{-1}$) and did not show the maximum in central Texas observed for the lower layer.

c. Precipitable water

The total precipitable water (PW) (mm) derived from VAS for 1648 and 2218 UTC is shown in Fig. 8. PW values in excess of 50 mm (2.0 in.) in extreme east Texas and Louisiana early in the afternoon had spread northward by the later time period. Meanwhile, decreasing PW occurred in central and southwest Texas. This change in moisture distribution is consistent with the LI changes described previously. Agreement of VAS PW with radiosonde-derived values (circled) was excellent, except that VAS overestimated the maximum in central Oklahoma by 10%–20%. The PW pattern does not relate well with the $6.7\text{-}\mu$ image (Fig. 5) because most PW is in the lower half of the troposphere, and the water vapor imagery reflects mid- and upper level moisture, with a peak response near 400 mb.

d. Mid-tropospheric moisture

A 500 mb relative humidity (RH) analysis at 2218 UTC which was manually computed from VAS temperatures and mixing ratios at that level is shown in Fig. 9. Because of the broad response of VAS moisture channels, this analysis is most representative of a layer-mean RH centered at 500 mb. Low RH (less than 30%) lay just to the south of DFW, increasing to around 50% to the northeast. The 500 mb RH at DFW was around 40%–45% based on these data. Confidence in these values is good based on comparisons with adjacent radiosonde data. Comparison of the RH field with the enhanced $6.7\text{-}\mu$ water vapor image in Fig. 5 shows good

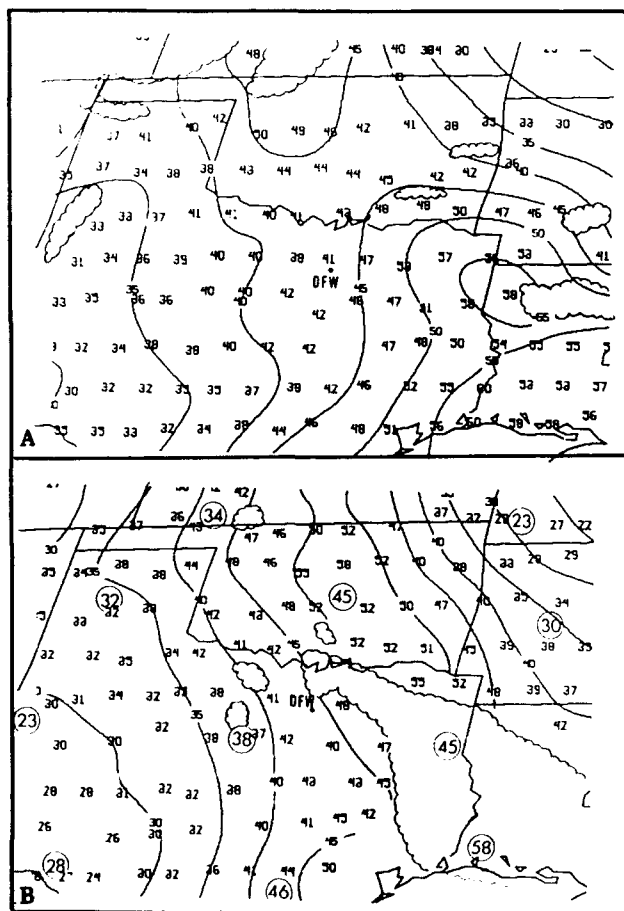


FIG. 8. As in Fig. 6 except VAS total precipitable water (PW) (mm).

qualitative agreement. Darker grey tones are seen to correspond to the lower RH values to the south of the DFW area and in southeast Oklahoma.

The presence of dry air aloft is important in areas of convection for two reasons: 1) Dry air overlying moist, unstable air results in potential (or convective) instability. When lifting occurs in such an environment, more rapid cooling of the dry air aloft results in destabilization and intense convection. Since the synoptic-scale forcing was weak on this day, this effect may have been minimal. 2) Another role of the dry air aloft could be to enhance downdrafts through evaporational cooling. Entrainment of midlevel (700 mb–400 mb) dry air is one of the factors proposed (along with precipitation loading and the melting of ice particles) as an initiating mechanism for the wet microburst (Caracena and Flueck 1987; McCarthy and Wilson 1984; Srivastava 1987).

e. Equivalent potential temperature

Horizontal fields of equivalent potential temperature θ_e (K) were produced for each pressure level that VAS sounding data were obtained. The θ_e is a conservative property for both moist and dry adiabatic processes. It is also proportional to the total static energy of an air parcel (Darkow 1968). Total static energy is the sum of sensible heat, latent heat, and geopotential energy.

An environment where θ_e decreases with height has the potential for strong convection because a parcel displaced vertically will become unstable (parcel θ_e is warmer than its surroundings) and will continue to accelerate. Conversely, a parcel of air descending in convective downdrafts will become cooler than the lower-level environment (negatively buoyant) and accelerate toward the surface. In the latter case, the kinetic energy of the parcel has increased at the expense of sensible heat (from evaporational cooling) and geopotential (due to sinking). Strong winds may result if the downdraft reaches the surface and is forced to spread radially. Entrainment of environmental air as the parcel descends reduces these effects somewhat. Caracena et al. (1986) determined the θ_e profile based on both the SEP radiosonde data and aircraft instrumentation around the time of the accident. Based on the kinetic energy generated from combined moist and dry descent, they estimated downdraft speeds of 35 m s^{-1} , close to the peak observed wind gust.

A regional analysis of the VAS low- to midlevel θ_e differential (TED) at 2218 UTC is shown in Fig. 10. A broad axis of maximum TED of 22 K extended from east Texas northwestward along the Red River into southwest Oklahoma. This indicates that the potential instability in this layer was similar over a fairly large area, not just in the vicinity of DFW. The maximum in southwest Arkansas is believed to be unreliable, due to the presence of low clouds which may have contaminated the retrievals. Except for the latter area, most convection occurred with values of TED ≥ 20 K. Surface wind damage associated with strong thunderstorms

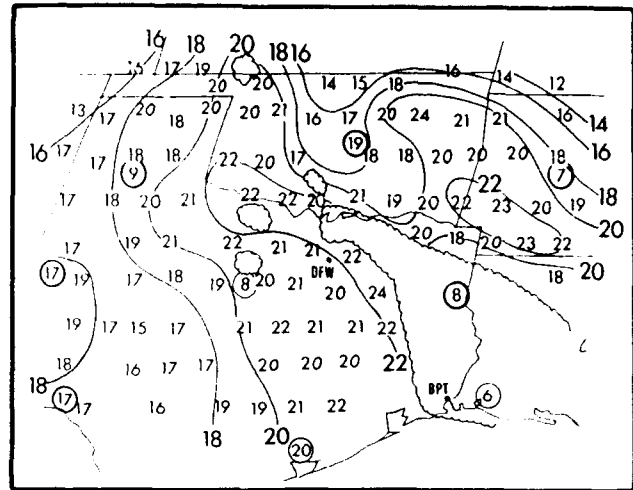


FIG. 10. VAS low- to midlevel θ_e differential (TED) (K) at 2218 UTC 2 August 1985. Radiosonde values are circled.

also occurred near Beaumont, Texas (BPT) that same afternoon (Storm Data 1985). The radiosonde-derived values of surface–700 mb TED (circled in Fig. 10) deviated considerably from VAS across much of northern Texas, as a result of the undetected moist layer near 700 mb. The VAS TED data shown appear to be more representative of a deeper layer (perhaps surface–600 mb) along this axis. The low- to upperlevel TED (not shown) had a similar pattern, and agreed better with the radiosonde data.

f. Vertical cross section

The vertical structure of static energy in north-central Texas on the afternoon of 2 August 1985 was examined by constructing a θ_e cross section. It has been shown that θ_e cross sections can be effectively used to delineate regions of potential instability in the preconvective environment (Mostek et al. 1986). The locations of VAS retrievals at 2218 UTC are shown in Fig. 11. The orientation of the cross section along the line A–B is roughly orthogonal to the flow at most levels.

The cross section (Fig. 12) shows the vertical decrease in θ_e (potential instability) becoming more concentrated (diminishing) below (above) 850 mb from east to west. The level of minimum θ_e descended from close to 500 mb in northeast Texas to near 700 mb in north-central Texas. This is significant in that potentially cool air was present relatively close to the surface in the DFW environment. The θ_e minimum near 700 mb was primarily a result of dryness, since temperatures were slightly warmer at that level in the west portion of the cross section. A cross section at 1648 UTC (not shown) indicated that the low-level moisture near DFW was shallower than at 2218 UTC and the dry zone aloft extended through a deeper layer but was slightly less pronounced. Although VAS cross sections are not routinely used operationally, a program which produces θ_e cross sections from radiosonde data on the

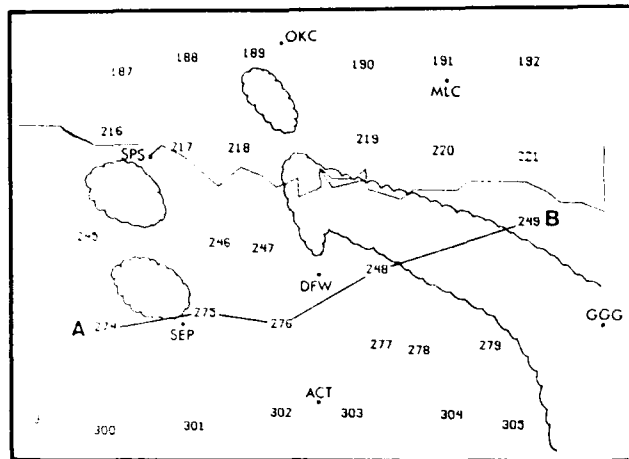


FIG. 11. Locations and identification numbers of VAS retrievals at 2218 UTC 2 August 1985, shown with respect to Dallas-Ft. Worth Airport (DFW). Other locations identified are Stephenville (SEP), Wichita Falls (SPS), Oklahoma City (OKC), McAlester (MLC), Longview (GGC), and Waco (ACT). Line A-B marks path of cross section in Fig. 12.

National Weather Service (NWS) Automation of Field Operations and Services (AFOS) system recently became available (Barker 1987).

g. Destabilization with time

With light south to southeast flow near the surface (Figs. 2 and 3), it would be expected that weak, positive

θ_e advection was occurring in the vicinity of DFW. The surface θ_e analysis for 1700, 2000, and 2300 UTC is shown in Fig. 13. The θ_e increased by 5 K in that period, mostly in the last 3 h, although the largest increases by far occurred in central Oklahoma. Between the times of the last two sets of VAS soundings, the 500 mb θ_e decreased approximately 1 K in the DFW area, resulting in an increase of 6 K in the potential instability. This is certainly not a dramatic change, but when added to the instability already present at the earlier retrieval time (16–18 K), it was significant.

The layer in which the most destabilization occurred in north-central Texas between 1648 and 2218 UTC was 850–700 mb. Fig. 14 shows the 850–700 mb θ_e change in 5.5 h derived from VAS, with a maximum of 5 K in a fairly large area centered on DFW. The secondary maximum over the Texas and Oklahoma panhandles was associated with isolated but vigorous thunderstorm development.

h. Air-mass analysis

The changes in stability across north-central Texas can be accounted for by examining some representative VAS retrievals. The value of VAS retrievals in analyzing differences in adjacent air masses has previously been demonstrated (Zehr et al. 1988). The comparison of soundings 248 and 276, located just to the northeast and southwest of DFW, respectively, is shown in Fig. 15. Temperatures were dry adiabatic up to about 700 mb, then nearly moist adiabatic up to the tropopause.

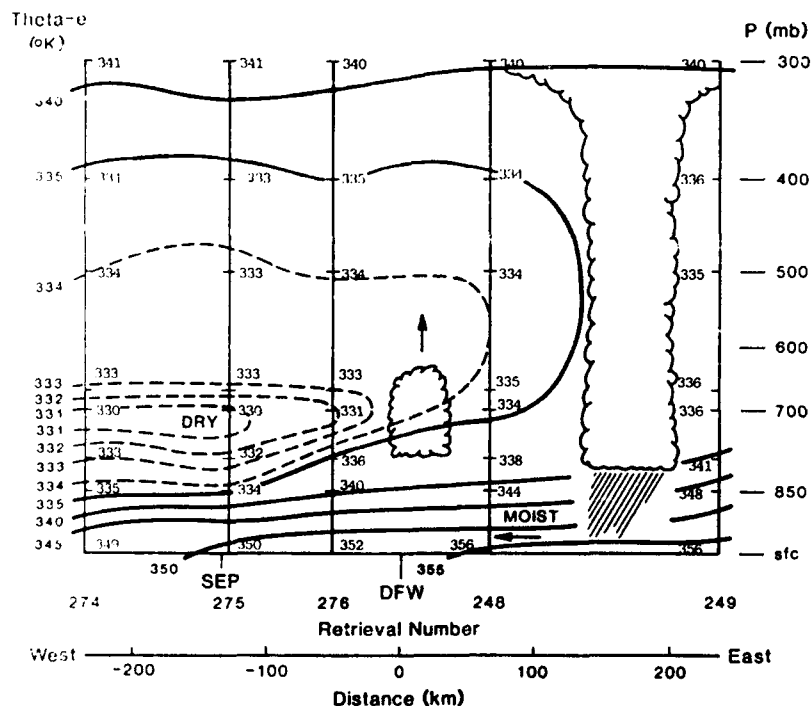
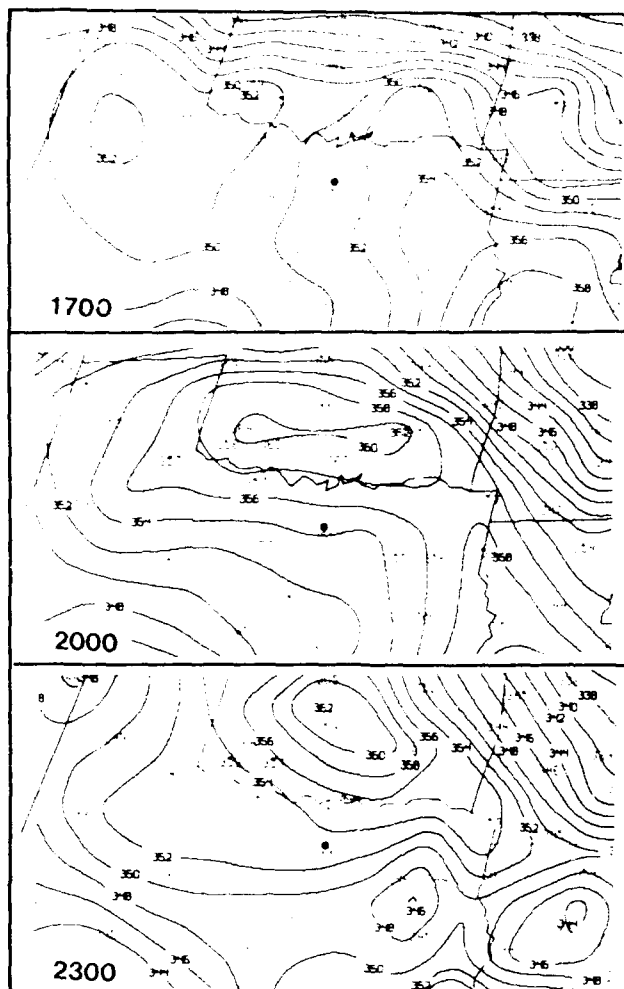


FIG. 12. Cross section of VAS equivalent potential temperature θ_e (K) at 2218 UTC along the line A-B in Figure 11. Scalloped borders represent approximate locations of convection.



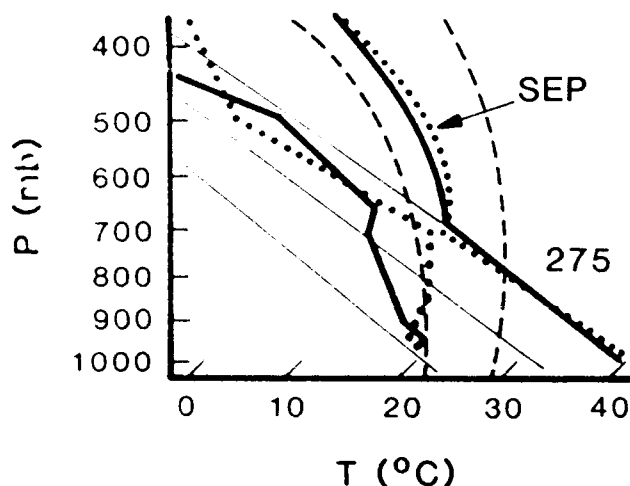


FIG. 16. Comparison of SEP radiosonde data at 0000 UTC (dotted) with adjacent VAS retrieval 275 at 2218 UTC (solid).

The DFW storm thus appeared to be a hybrid type of microburst storm. It had some characteristics similar to those in the Rocky Mountains which result in dry microbursts (high cloud bases, dry subcloud region, and a midlevel moist layer). At the same time, some features relevant to wet microbursts were also present (heavy rain, lightning, and dry midtropospheric air). Similar findings were obtained in studies of other microburst events in the southern Plains (Read et al. 1987) and in a multiscale analysis of the DFW storm (Caracena et al. 1986). A composite of the three basic types of microburst environments is shown in Fig. 17.

The higher thunderstorm tops to the northeast of DFW are attributed to more ample subcloud moisture present, as shown in Fig. 15. The more humid environment resulted in larger positive buoyancy in the mid- and upper levels. Slightly warmer temperatures above cloud base, coupled with drier sub-cloud conditions (both seen to some extent in the VAS data), inhibited thunderstorm growth southwest of DFW. The VAS mixing ratios in the lowest layer increased from $12\text{--}13\text{ g kg}^{-1}$ southwest of DFW to a maximum of over 17 g kg^{-1} in southern Oklahoma (Fig. 18). Mixing ratios derived from surface data at 2200 UTC fluctuated considerably due to local variations in T and T_d .

The DFW area thus appeared to be in just the right location with respect to favorable microburst conditions. The subcloud air was dry, yet sufficiently moist for convection, and midlevel stability was decreasing as hot, unstable, low level air parcels moved northward. Dry air at midlevels was also present to enhance evaporational cooling above cloud base.

i. Vertical energy profile at DFW

The vertical θ_e profile interpolated from VAS soundings 248 and 276 at 2218 UTC (A) is shown in Fig. 19. Also shown for comparison are the θ_e profiles for the SEP radiosonde (B), and the VAS-derived profile for the Monrovia microburst storm (Fujita 1988) which occurred on 20 July, 1986 (C). The Monrovia storm could also be considered small in size in the severe storm spectrum, yet caused considerable surface wind damage. The Monrovia storm also developed with weak or nonexistent synoptic-scale forcing under an upper-level anticyclone. The θ_e is observed to decrease rapidly with height for profiles A and C. The SEP profile decreased less rapidly with height from the surface to 700 mb, due to the shallow moist layer aloft, but had a lower θ_e minimum than VAS, located just above 700 mb. For the DFW storm, θ_e increased slowly from 700 mb to about 400 mb because of the moist adiabatic lapse rate and minimal moisture in this layer. In reality, this decrease may have occurred in a very shallow layer, as suggested by profile B. The magnitude of vertical θ_e differential (TED) was similar for all three profiles. It is easy to see that an air parcel forced to ascend in such an environment would encounter no opposition. When more extensive data are obtained for wet microburst events, it would be useful to derive a composite θ_e profile for comparison studies and possibly even for short-range forecast applications.

j. Buoyant energy

Buoyant energy analyses were derived from the VAS retrievals using programs originally developed for the PRE-STORM mesoscale project in Oklahoma (Zehr et al. 1988). The use of layer averages of temperature and lowest-kilometer mixing ratio in these calculations minimizes the main weakness of VAS soundings—poor vertical resolution. The amount of positive buoy-

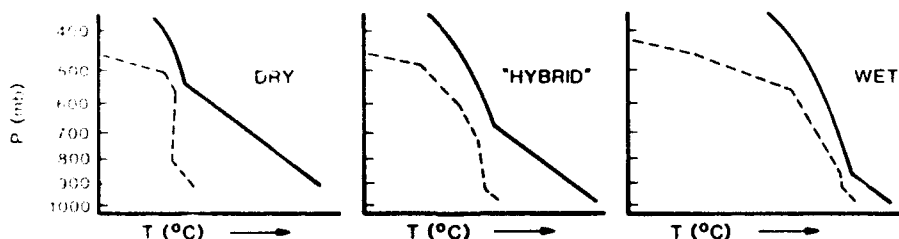


FIG. 17. Representative soundings for dry (left), hybrid (center) and wet (right) types of microburst environments.

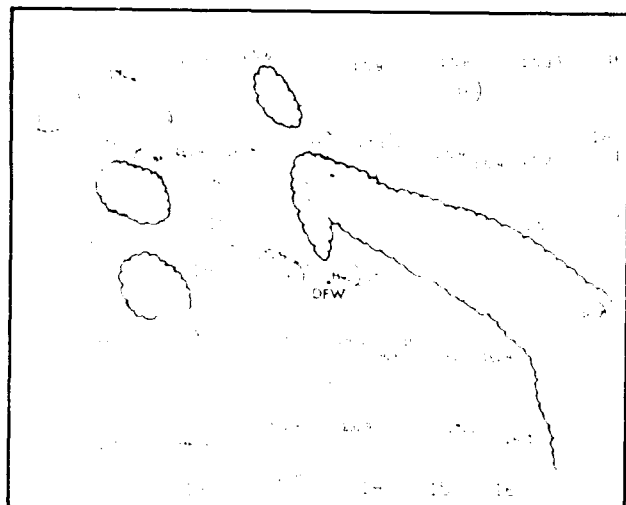


FIG. 18. Lowest layer VAS mixing ratios (g kg^{-1}) over north-central Texas and southern Oklahoma at 2218 UTC. Mixing ratios determined from some surface reports are circled. Although the VAS values are derived from surface data, they present a more consistent analysis.

ant energy (PBE) present in a sounding is the area between the moist adiabatic temperature profile of a saturated, rising air parcel and the environmental temperature profile, between the level of free convection (LFC) and the equilibrium level (EL). Negative buoyant energy (NBE) is the energy required for a parcel to overcome any stability present below cloud base in order to reach the LFC. Overcoming a negative energy layer in the sounding may be accomplished by either heating or forced ascent. The interpolated VAS sounding for DFW at 2218 UTC is shown in Fig. 20, along with a depiction of the NBE and PBE present in the sounding. The NBE area is enlarged slightly for display. It can be seen that considerable energy is available for strong thunderstorm updrafts.

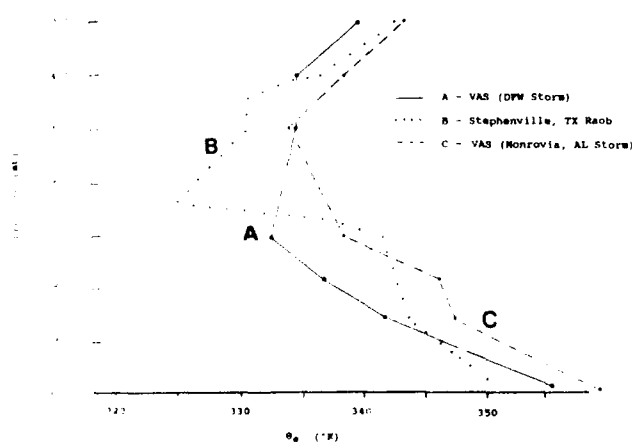


FIG. 19. Vertical profiles of θ_e (proportional to total static energy) for (a) the DFW storm interpolated from VAS retrievals 248 and 276 at 2218 UTC, (b) the SEP radiosonde, and (c) the VAS data for the Monrovia, Alabama storm on 20 July 1986.

The PBE and NBE values (J kg^{-1}) for northeast Texas and southern Oklahoma derived from VAS at 1648 and 2218 UTC are shown in Fig. 21. For comparison, a visible image at 2301 UTC for the same area is shown in Fig. 22. Maximum PBE at the latter time is observed near DFW and in southeast Oklahoma. A rapid decrease in PBE occurs to the south and west of DFW, corresponding to the region of midlevel warming and low-level drying observed in Fig. 15. This PBE gradient also supports the "underrunning" concept and the cloud top height differences described earlier.

The combination of large PBE and minimal NBE values near DFW and in southeast Oklahoma indicated that strong convection was likely in these areas. Vigorous cells are developing near MLC in Fig. 22. The relatively low lapse rates (Fig. 7) would seem to eliminate southeast Oklahoma as a strong candidate for microbursts, however. Some of the high PBE areas appear to be cloud free. This is likely a result of some undetected low-level stability present in these areas, probably a result of thunderstorm-generated meso-highs. The fairly large area sampled by VAS is also a factor.

Fig. 21 shows that earlier in the afternoon, NBE exceeded PBE by a substantial amount near DFW, while the reverse was true to the southeast (near GGG), where the deep convective cells first formed. The buoyant energy appeared to best delineate the potential areas of very strong convection of all the VAS analyses presented so far.

6. Surface forcing mechanism

The mere presence of strong instability and positive buoyancy does not, of course, guarantee that strong

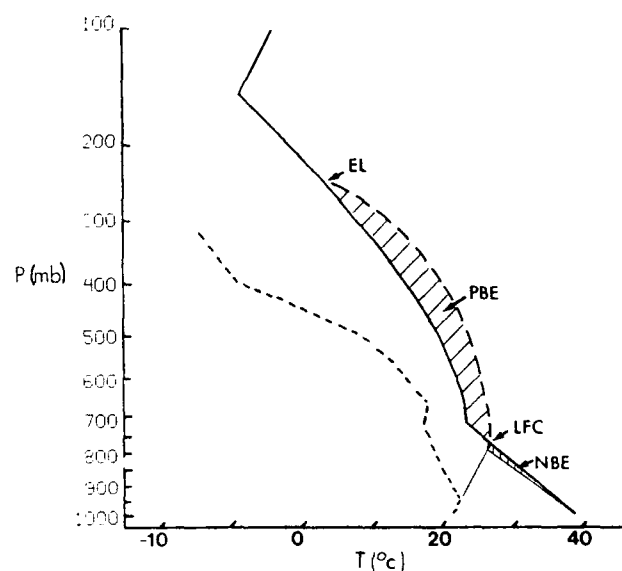


FIG. 20. The VAS sounding at DFW interpolated from retrievals 248 and 276 at 2218 UTC, showing the area of positive buoyant energy (PBE), total negative buoyant energy (NBE), the level of free convection (LFC) and the equilibrium level (EL). The NBE area is enlarged slightly for better visibility.

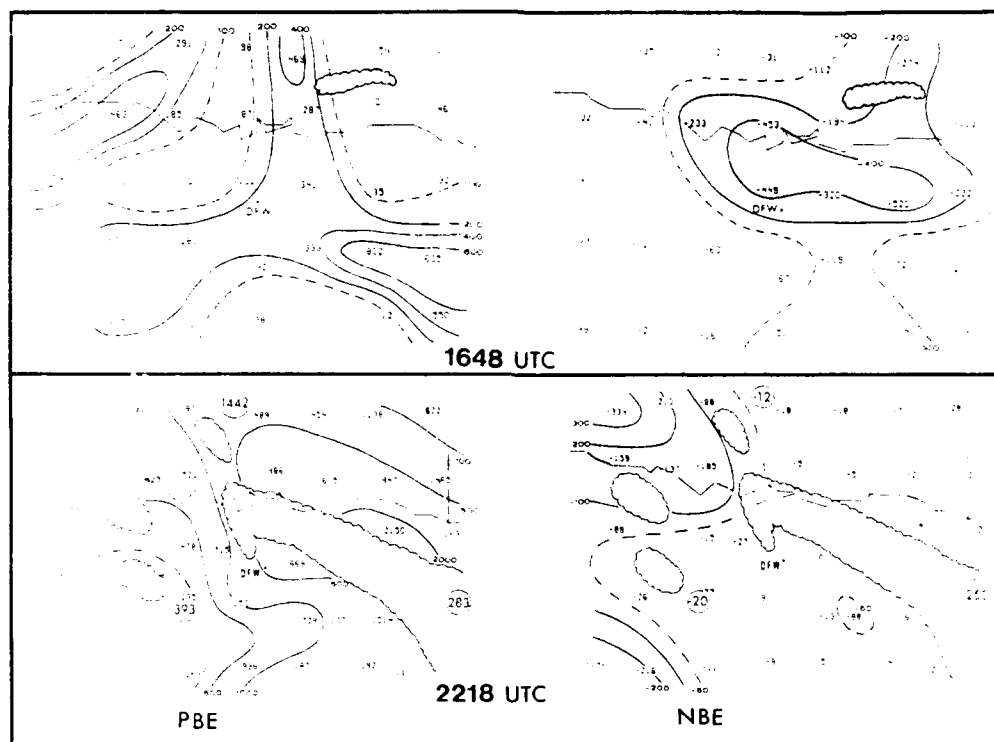


FIG. 21. (left) Analyses of PBE and (right) NBE (J kg^{-1}) at (top) 1648 UTC and (lower) 2218 UTC. Values at radiosonde sites are circled on the 2218 UTC analysis.

thunderstorms will occur. Fig. 22 shows that although most convection occurred within the area of maximum LI, PW, TED, and PBE (Fig. 6, 8, 10 and 21), portions of the region have little or no activity. Since the synoptic-scale forcing was weak or nonexistent, a local surface-lifting mechanism must have been present.

Low-level convergence along both the quasi-stationary front (Fig. 3) and the outflow boundary in the Dallas-Ft. Worth area (Fig. 4) provided such a mechanism.

Surface winds were generally light over the Southern Plains on 2 August 1985, resulting in weak, poorly defined divergence patterns. The regional divergence

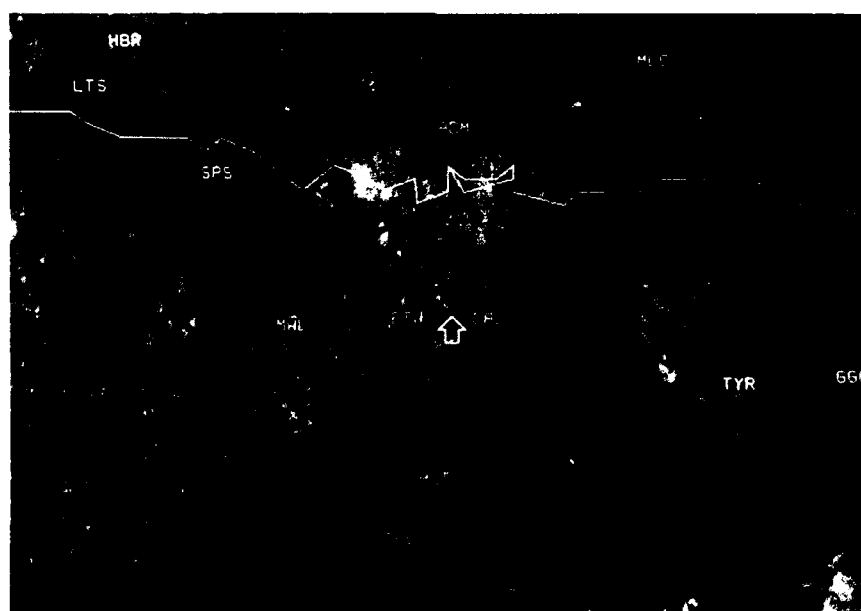


FIG. 22. GOES visible image at 2301 UTC 2 August 1986 for approximately the same area as Fig. 21.

analyses at 1800, 2100, 2200, and 2300 UTC are shown in Fig. 23. An axis of convergence extending from southwest Louisiana to extreme southeast Oklahoma at 1800 UTC was observed to shift westward through the period, settling in over the Dallas-Ft. Worth area by 2300 UTC. Convergence was first evident from the surface winds at 2200 UTC, although the maximum in the contour analysis is well to the east, apparently influenced heavily by a southwest wind at a station in east Texas.

Surface divergence is a highly scale-dependent phenomenon which is related to the density of available wind data and grid spacing at which the calculations are made. The magnitude of convergence in the regional analyses was a maximum of about $15 \times 10^{-6} \text{ s}^{-1}$. The surface convergence at DFW was also estimated using a time to space conversion of the winds at the DFW airport centered on 2300 UTC. The convergence obtained with this approach was $\approx 2 \times 10^{-3} \text{ s}^{-1}$, fully two orders of magnitude higher than the larger scale analysis. Convergence of this extent would have been sufficient to generate a 2 m s^{-1} updraft at 1 km above ground. This is weaker, but similar in magnitude to lifting observed by aircraft along stronger thunderstorm outflows (Purdum and Sinclair 1988).

7. Conclusions

The VAS analyses indicated the presence of several conditions which would have been helpful in suspecting

north central Texas as a region of possible microburst activity: 1) the large subcloud lapse rate, particularly from 850 to 700 mb; 2) the large horizontal stability gradient, which slowly increased with time; 3) midlevel capping just to the south of DFW, caused by slightly warmer (2°C) temperatures at 500 mb; but 4) strong positive buoyant energy above cloud base near DFW; and 5) an adjacent pocket of midlevel dry air. On this particular day, these conditions were clearly shown only by the last set of VAS sounding retrievals (2218 UTC) which would have been too late to be of much use operationally. While VAS and conventional surface reports indicated that thunderstorm activity was likely in the DFW area, it is apparent that no single VAS-derived field could have predicted the severe microburst that occurred. However, a combination of the VAS analyses, satellite imagery, and surface data, would have indicated the likelihood of a microburst event. Specifically, the intersection of areas of high lapse rates, high net buoyancy ($\text{PBE} + \text{NBE}$), midlevel dry air, and surface convergence successfully isolated the DFW region as a prime candidate. Fig. 24 schematically shows the relationship of these parameters for the 2200–2300 UTC period.

Comparison of VAS-derived data with radiosonde data indicated favorable agreement, especially for the layer-integrated quantities such as lifted index, precipitable water and buoyant energy analyses. The chief benefit of the VAS data evident from this case is the

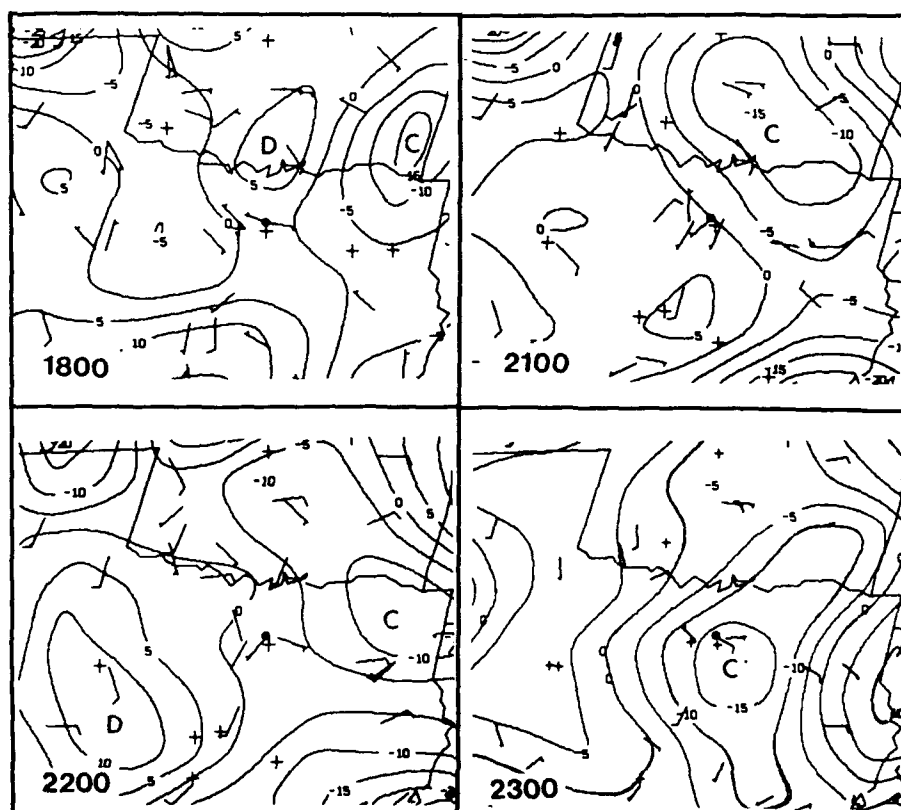


FIG. 23. Surface divergence ($\times 10^{-6} \text{ s}^{-1}$) at 1800, 2100, 2200, and 2300 UTC 2 August 1985. DFW is located at the large dot.

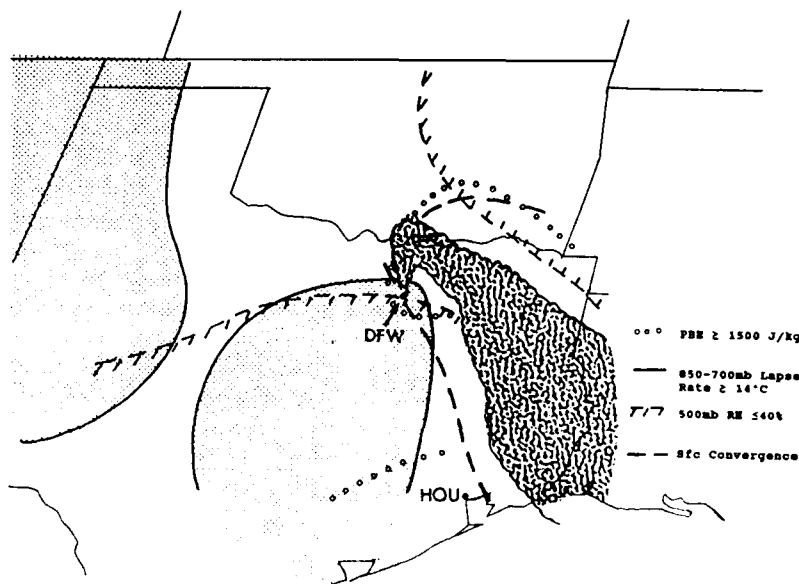


FIG. 24. Composite schematic of VAS-derived fields and the location of maximum surface convergence around 2200–2300 UTC 2 August 1985.

better spatial definition of both of maxima and gradient regions than can be obtained from the radiosondes.

Only two types of analyses derived from VAS sounding data are currently available operationally (LI and PW), but only to certain national forecast centers. Water vapor images also provide a qualitative estimate of the locations of upper-level dry zones. Water vapor imagery is currently produced hourly, although in August, 1985 only 6-h images were available at NWS forecast offices.

Based on this study, several other VAS-derived parameters would be desirable in the operational forecast environment to aid in the short-range forecasts of areas of possible microburst activity. These are net buoyant energy, lapse rates, and layer mean RH at midlevels. It was also seen that individual VAS profiles are invaluable in detecting variations in air mass characteristics within a short distance, although absolute values of low-level moisture should be suspect. The vertical θ_e difference (TED) is useful in identifying areas of strong convective instability, but for the DFW case at least, this parameter did not seem to provide any information which would differentiate areas of high microburst risk.

Some of the difficulties previously noted with the current VAS sounding system (erratic frequency, poor vertical resolution, difficulty with cloudy regions) will show improvements in the near future. The nested grid model (NGM), which has higher vertical layer resolution than the LFM, has already been installed as the source of first-guess data fields. The GOES I-M sounders will have six additional IR channels, resulting in a slight improvement in vertical resolution. More importantly, however, the sounder will be independent from the imager, allowing uninterrupted time series of

vertical profiles. The higher resolution of IR channels and the presence of a visible channel with the GOES I-M sounders will permit better cloud screening, resulting in a larger number of good quality retrievals.

Other new remote sensing systems will soon provide data which will complement VAS soundings in the detection of mesoscale severe storm events such as microbursts. A Doppler weather radar system known as NEXRAD (next-generation radar) will become operational in the 1990s (e.g., Milner 1986). In addition to depicting intense precipitation echoes, the radar will allow frequent analyses of low-level flow features important in aviation operations, such as strong outflow centers which result in microbursts, gust fronts and mesocyclones related to tornadoes. On a smaller scale, the terminal Doppler weather radar (TDWR) will detect these hazards in the airport environment and provide automatic warnings to flight controllers (Turnbull et al. 1989). Also, atmospheric profilers will produce frequent, high-resolution vertical wind profiles deduced from the motion of aerosols. Profilers will result in more accurate location of important upper-flow features which may trigger convection and will help to define the magnitude of the vertical shear. A demonstration network of 31 profilers is expected to be in place by mid-1990 in the central United States.

By similar analysis of a larger number of these small, intense convective storms, it is hoped that enough data can be obtained to estimate the *probability* of such an event occurring within a short time span (several hours). Despite their shortcomings, VAS soundings appear to be useful for this purpose, given their ability to diagnose short-term temporal and spatial changes in atmospheric environmental conditions.

Acknowledgments. The data used in this study were collected while the author was visiting the Cooperative Institute for Meteorological Satellite Studies (CIMSS) at the University of Wisconsin. Gary Wade assisted in the collection and interpretation of the data. Thanks to Fran Holt and Dr. Paul Menzel of NESDIS and Phil Bothwell and others at the NWS Southern Region Headquarters for their helpful comments. Paige Bridges drafted some of the figures and Gene Dunlap provided photographic help.

REFERENCES

- Barker, T. 1987. Convective spatial cross sections. AFOS Program Note, National Weather Service Western Region Headquarters, Salt Lake City, Utah.
- Caracena, F., and J. A. Flueck. 1987. Forecasting and classifying microburst activity in the Denver area subjectively and objectively. AIAA 25th Aerospace Sciences Meeting, Reno, NV, January 12–15, 1987.
- , R. Ortiz and J. A. Augustine. 1986. The crash of Delta Flight 191 at Dallas–Fort Worth International Airport on 2 August 1985: Multi-scale analysis of weather conditions. NOAA Technical Report ERL 430-ESG 2, Environmental Science Group, Boulder, CO.
- Carlson, T. N., S. G. Benjamin, G. S. Forbes and Y.-F. Li. 1983. Elevated mixed layers in the regional severe storm environment. Conceptual models and case studies. *Mon. Wea. Rev.* **111**: 1453–1473.
- Darkow, G. L. 1968. The total energy environment of severe storms. *J. Appl. Meteor.* **2**: 199–205.
- Fujita, T. T. 1983. Microburst wind shear at New Orleans International Airport, Kenner, Louisiana on July 9, 1982. *SMRP Research Paper 199*, University of Chicago, 39 pp.
- . 1986. DFW microburst on August 2, 1985. *SMRP Research Paper 217*, University of Chicago, Illinois.
- . 1988. Monrovia microburst of 20 July 1986: A study of “SST.” Proc. of AMS 15th Conf. on Severe Local Storms, February 22–26, 1988, Baltimore, MD, 380–383.
- , and F. Caracena. 1977. An analysis of three weather-related accidents. *Bull. Amer. Meteor. Soc.* **58**: 1164–1181.
- Hasler, A. F., R. Mack and A. Negri. 1982. Stereoscopic observations from meteorological satellites. Proc. of the COSPAR 24th Plenary Meeting, Ottawa, Canada. Maryland: NASA/Goddard Space Flight Center.
- Hayden, C. M., W. P. Menzel and A. J. Schreiner. 1984. The clouds and VAS. Conference on Satellite/Remote Sensing and Applications, June 25–29, 1984, Clearwater, Florida. AMS Preprint pp 49–54. Boston: American Meteorological Society.
- Kitzinger, D. H., and W. E. McGovern. 1988. Objective assessment of 1984–85 VAS products as indices of thunderstorm and severe storm potential. NOAA Technical Memo NWS TDL 78. Techniques Development Laboratory, Silver Spring, MD.
- Komajda, R. J., and K. McKenzie. 1987. The GOES I-M imager and sounder instruments and the GVAR retransmission format. NOAA Technical Report NESDIS 33. U.S. Dept. of Commerce, Washington, DC.
- Mack, R. A., A. F. Hasler and E. B. Rodgers. 1982. Stereoscopic observations of hurricanes and tornadic thunderstorms from geostationary satellites. Proc. of the COSPAR 24th Plenary Meeting, Ottawa, Canada. Maryland: NASA/Goddard Space Flight Center.
- McCarthy, J., and J. W. Wilson. 1984. The microburst as a hazard to aviation. Proc. Nowcasting-II Symposium, Norrköping, Sweden, 3–7 September, 1984. Paris: European Space Agency, 21–30.
- Menzel, P., and C. Hayden. 1986. Description of VAS Processing Techniques. Joint In-house publication, Satellite Applications Laboratory and Cooperative Institute for Meteorological Satellite Studies, University of Wisconsin, Madison.
- , T. H. Achtor, C. Hayden and W. Smith. 1983. The advantages of sounding with the smaller detectors of the VISSR Atmospheric Sounder. NOAA Technical Memo NESDIS 6. Washington, D.C.
- Mills, G. A., and C. M. Hayden. 1983. The use of high horizontal resolution satellite temperature and moisture profiles to initialize a mesoscale numerical model—a severe weather case study event. *J. Clim. and Appl. Meteor.* **22**: 649–663.
- Milner, S. 1986. NEXRAD—The coming revolution in radar storm detection and warning. *Weatherwise* **39**: 72–85.
- Montgomery, H. E., and L. W. Uccellini, Ed. 1985. VAS demonstration (VISSR Atmospheric Sounder) description and final report. NASA Reference Publication 1151. Goddard Space Flight Center, Greenbelt, MD.
- Mostek, A., L. W. Uccellini, R. A. Petersen and D. Chesters. 1986. Assessment of VAS soundings in the analysis of a preconvective environment. *Mon. Wea. Rev.* **114**: 62–87.
- Petersen, R. A., L. W. Uccellini, A. Mostek and D. Chesters. 1984. Delineating mid- and low-level water vapor patterns in preconvective environments using VAS moisture channels. *Mon. Wea. Rev.* **112**: 2178–2198.
- Proctor, F. H. 1988. Numerical simulations of the 2 August 1985 DFW Microburst with the three-dimensional Terminal Area Simulation System. Preprint Volume, 8th Conference on Severe Local Storms, Baltimore, MD.
- Purdom, J. F. W. 1971. Satellite imagery and severe weather warnings. 7th Conf. on Severe Local Storms, Kansas City, Missouri. AMS Preprint, pp 120–137. Boston: American Meteorological Society.
- , and P. C. Sinclair. 1988. Dynamics of convective scale interaction. Proc. of AMS 15th Severe Local Storms Conference, February 22–26, 1988, Baltimore, MD. AMS Preprint, 354–359.
- Read, W. L., C. J. Sohl, M. L. Branick and J. C. Lowery. 1987. Observed microbursts in the NWS Southern Region during 1986. NOAA Technical Memorandum NWS SR-121. Scientific Services Division, Southern Region. Ft. Worth, Texas.
- Smith, W. L. 1983. The retrieval of atmospheric profiles from VAS geostationary radiance observations. *J. Atmos. Sci.* **40**: 2025–2035.
- , and H. Woolf. 1984. Improved vertical soundings from an amalgamation of polar and geostationary radiance observations. Conf. on Satellite Meteorology/Remote Sensing and Applications, Clearwater, FL, Amer. Meteor. Soc., Boston, 45–48.
- , V. E. Suomi, F. X. Zhou and W. P. Menzel. 1982. Nowcasting applications of geostationary satellite atmospheric sounding data. *Nowcasting*. London: Academic Press.
- Srivastava, R. C. 1987. A model of intense downdrafts driven by the melting and evaporation of precipitation. *J. Atmos. Sci.* **44**: 1752–1773.
- Storm Data. 1985. Vol. 27, No. 8, August, 1985, National Climatic Data Center, NOAA, Asheville, North Carolina.
- Suomi, V. E., R. Fox, S. S. Limaye and W. L. Smith. 1983. McIDAS III: A modern interactive data access system. *J. Appl. Meteor.* **22**: 766–778.
- Turnbull, D., J. McCarthy, J. Evans and D. Zrnic. 1989. The FAA Terminal Doppler Weather Radar Program (TDWR) program. Proc. of the 3rd Inter. Conf. on the Aviation Weather System, 30 January–3 February 1989, Anaheim, California. Amer. Meteor. Soc., Boston, 414–419.
- Wade, G. S., A. L. Siebers and R. W. Anthony. 1985. An examination of current atmospheric stability and moisture products retrieved from VAS measurements in real-time for the NSSFC. Proc. of AMS 14th Conf. on Severe Local Storms, October 29–November 1, 1985, Indianapolis, Indiana, 105–108.
- Wakimoto, R. M. 1985. Forecasting dry microburst activity over the High Plains. *Mon. Wea. Rev.* **113**: 1131–1143.
- Zehr, R. M., J. F. W. Purdom, J. F. Weaver and R. N. Green. 1988. Use of VAS data to diagnose the mesoscale environment of convective storms. *Wea. Forecasting* **3**: 33–49.